



## Enhanced photocatalytic performance of silver-based solid solution heterojunctions prepared by hydrothermal method

Maocai Zhang, Shifeng Zhao, Qingshan Lu\*

School of Physical Science and Technology and Inner Mongolia Key Laboratory of Nanoscience & Nanotechnology, Inner Mongolia University, Hohhot 010021, China



### ARTICLE INFO

#### Keywords:

Phase transformation  
Light response  
Heterojunction  
Charge carrier

### ABSTRACT

Silver-based solid solution with phase heterojunctions ( $\alpha/\beta$ -AgAl<sub>0.4</sub>Ga<sub>0.6</sub>O<sub>2</sub> heterostructure) was fabricated through phase transformation under hydrothermal treatment. X-ray diffraction and Raman spectra showed the phase transformation behavior, phase structure and composition of the samples. Transmission electron microscopy illustrated the mixed morphology of near-spherical  $\beta$  phase together with platelet  $\alpha$  phase and the formation of phase heterojunctions. UV-vis absorption edges of the  $\alpha/\beta$ -AgAl<sub>0.4</sub>Ga<sub>0.6</sub>O<sub>2</sub> heterostructure were adjusted from 470 to 515 nm by controlling phase ratio under different hydrothermal temperatures. The heterostructure displayed the enhanced photocatalysis activity for the degradation of methyl orange in comparison to single  $\alpha$  or  $\beta$  phase. In addition, electrochemical properties including small diameter of the arc radius and maximum photocurrent indicated high separation and fast transfer efficiency of the photoinduced carriers across the phase heterojunctions. Therefore, both of the enhanced utilization of visible light and efficient carrier separation of  $\alpha/\beta$ -AgAl<sub>0.4</sub>Ga<sub>0.6</sub>O<sub>2</sub> heterostructure contributed to its excellent photocatalysis property.

### 1. Introduction

In view of environmental pollution concerns, semiconductor photocatalysis as a green chemical technique has emerged as one of the most promising technologies because it represents an easy way to utilize either natural sunlight or artificial indoor illumination [1,2]. Up to now, various semiconductors have been developed to meet the requirements for their practical application, such as TiO<sub>2</sub> [3], ZnO [4,5], Ag<sub>3</sub>PO<sub>4</sub> [6,7], CdS [8], C/CuO@g-C<sub>3</sub>N<sub>4</sub> [9] and so on. However, the photocatalytic efficiency of these traditional photocatalysts is still low, which are mainly induced by weak light absorption in term of narrow response for visible light and fast recombination of photoexcited electrons and holes. To overcome these drawbacks, a great number of methodologies have been proposed to develop photocatalysts with visible-light response and high photo-quantum efficiency, including metal or non-metal ions doping, heterostructure, dye sensitization and so on [10–13]. Among them, the semiconductor heterojunction photocatalysts have received great interest, because the bandgap overlap of heterostructure can expand the visible light absorption by controlling the phase component. Meanwhile, the internal electric field built from the matched band structures provides the driving force to accelerate carrier separation and transfer, endowing the photocatalysts with excellent photocatalytic performance [2,4,8]. For instance, Juntrapirom and co-workers constructed SnS/BiOI heterostructure to improve the

visible light photocatalytic efficiency [14]. Khedr et al. synthesized highly active mixed phase TiO<sub>2</sub> [15]. Nagajyothi et al. utilized a green chemical method to prepare Ag/g-C<sub>3</sub>N<sub>4</sub> composites which showed higher photocatalytic activity than pure g-C<sub>3</sub>N<sub>4</sub> in the degradation of malachite green [16]. In particular, considerable researches recently have demonstrated that the mixed phase heterojunctions in semiconductors could be beneficial for enhancing the photocatalytic activity [17–19].

Solid solution photocatalysts with adjustable electronic structure and continuous band gaps have focused on extensive concentration for their high visible light activity. In previous studies, element substitution was widely explored such as MCo<sub>1/3</sub>Nb<sub>2/3</sub>O<sub>3</sub> (M = Ca, Sr, and Ba) and In<sub>0.8</sub>M<sub>0.2</sub>TaO<sub>4</sub> (M = 3d transition metals) [20,21]. However, it is not accurate to adjust the electronic structures. As a special semiconductor, silver-based solid solution AgAl<sub>1-x</sub>Ga<sub>x</sub>O<sub>2</sub> with delafossite structure has attracted great attention due to their hybridization of Ag5s5p, Al3s3p and Ga4s4p states in the conduction band [22]. Thus, the bandgap together with the visible light absorption behavior can be easily tailored by the elementary composition. Besides, the silver-based solid solution includes two polymorphs:  $\alpha$  phase (3R) and  $\beta$  phase (2H) [23]. To achieve high photocatalytic activity, the design and fabrication of efficient phase heterojunctions for AgAl<sub>1-x</sub>Ga<sub>x</sub>O<sub>2</sub> become very important. In our reported work, the mixed phase  $\alpha/\beta$ -AgAl<sub>0.4</sub>Ga<sub>0.6</sub>O<sub>2</sub> with enhanced photocatalytic activity was for the first time synthesized

\* Corresponding author.

E-mail address: [luqs@imu.edu.cn](mailto:luqs@imu.edu.cn) (Q. Lu).

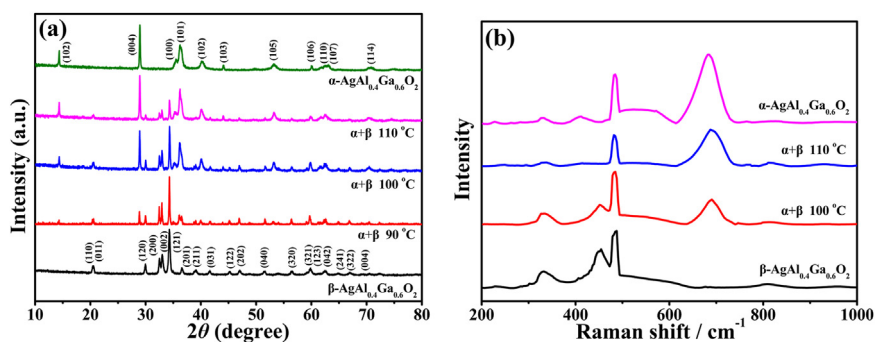


Fig. 1. XRD patterns (a) and Raman spectra (b) of the  $\alpha/\beta$ - $\text{AgAl}_{0.4}\text{Ga}_{0.6}\text{O}_2$  heterostructure with different hydrothermal temperatures.

by hydrothermal method [24]. However, the phase component of heterostructure is not well controlled by changing the hydrothermal time. More importantly, the behavior of photogenerated carrier related to phase heterojunctions has not been deeply studied up to now.

In this work, we have improved the hydrothermal method to fabricate silver-based solid solution with phase heterojunctions ( $\alpha/\beta$ - $\text{AgAl}_{0.4}\text{Ga}_{0.6}\text{O}_2$  heterostructure) by controlling the phase transition temperature. The phase transformation behavior, microstructure and UV-vis absorption of the samples are investigated. All the  $\alpha/\beta$ - $\text{AgAl}_{0.4}\text{Ga}_{0.6}\text{O}_2$  heterostructure shows higher photocatalytic activity than the single  $\alpha$  or  $\beta$  phase. An in-depth understanding of improved carrier separation efficiency ascribed to the phase heterojunctions is verified by electrochemical properties.

## 2. Experimental section

### 2.1. Synthesis

Single phase  $\beta$ - $\text{AgAl}_{0.4}\text{Ga}_{0.6}\text{O}_2$  was firstly prepared as the procedures in our reported work [25].  $\alpha/\beta$ - $\text{AgAl}_{0.4}\text{Ga}_{0.6}\text{O}_2$  heterostructure with different phase components was obtained under hydrothermal treatment by controlling temperature. The details were as follows: 0.6 g of the obtained  $\beta$ - $\text{AgAl}_{0.4}\text{Ga}_{0.6}\text{O}_2$  was dispersed into 40 mL of deionized water. After ultrasonic dispersion for 30 min, the suspension was transferred into a Teflon-lined stainless autoclave and kept at certain temperature varying from 90° to 130°C for 5 h. Finally, the products were cooled naturally, filtered, washed with distilled water and dried at room temperature. The  $\alpha/\beta$ - $\text{AgAl}_{0.4}\text{Ga}_{0.6}\text{O}_2$  heterostructure was obtained.

### 2.2. Characterization

Phase structure was investigated on PANalytical Empyrean X-ray diffractometer using  $\text{Cu K}\alpha$  radiation in  $\theta$ - $2\theta$  scan mode at 40 kV and 40 mA. Raman analysis was carried out on a Renishaw InVia Raman spectrometer with the green line of an Ar-ion laser (514.5 nm) in micro-Raman configuration. Transmission electron microscopy (TEM) was carried out with a JEM-2010 transmission electron microscope operating at 200 kV. X-ray photoelectron spectroscopy (XPS) measurements were performed on Kratos Amicus using  $\text{Mg K}\alpha$  as X-ray source. The energy scale was internally calibrated by referencing to the binding energy of the C 1 s peak of a carbon contaminant at 284.6 eV. UV-visible absorption spectra (UV-vis) were obtained using a Hitachi U-3900 UV-vis spectrophotometer. Electrochemical impedance spectroscopy (EIS) and photocurrent response spectroscopy (PRS) were conducted on a CHI-660E electrochemical system with a three-electrode cell.

### 2.3. Photoelectrochemical and photocatalytic properties

EIS measurements were tested in a conventional three electrode system using 0.1 M  $\text{Na}_2\text{SO}_4$  as electrolyte, a platinum wire as a counter electrode and  $\text{Ag}/\text{AgCl}$  as a reference electrode. The working electrodes were prepared as follows: 5 mg of the as-prepared sample was dispersed in 375  $\mu\text{L}$  of distilled water, 125  $\mu\text{L}$  of ethyl alcohol and 25  $\mu\text{L}$  of nafion perfluorinated resin solution to form a suspension. 4  $\mu\text{L}$  of the suspension was coated onto the glassy carbon electrode with a diameter of 3 mm and then dried in air.

Photocurrent spectra were carried out in a three electrode electrochemical cell using 0.1 M  $\text{Na}_2\text{SO}_4$  as electrolyte, Pt foil as a counter electrode and  $\text{Ag}/\text{AgCl}$  as a reference electrode. The working electrodes were prepared as follows: 10 mg of the as-prepared sample were dispersed in 0.4 mL ethyl alcohol and deionized water to form a suspension, which was then coated onto a 0.5  $\text{cm}^2$  ITO glass and annealed at 120 °C for 5 h in vacuum.

The photocatalytic performance of the samples was evaluated by MO degradation through a photochemical reactor. 0.3 g of the photocatalyst was dispersed in 300 mL MO aqueous solution with a concentration of 10 mg/L. Prior to irradiation, the suspensions were magnetically stirred in the dark for 60 min to reach a adsorption equilibrium of MO on the photocatalyst. Subsequently, the suspension was exposed to visible light irradiation ( $\lambda > 420 \text{ nm}$ ) under a Xe lamp of 50 W. At a certain time interval, 3 mL of the suspension was withdrawn and centrifuged. The supernatant was analyzed by UV-vis spectrophotometer.

## 3. Results and discussion

Fig. 1a shows the XRD patterns of the samples hydrothermally treated under different temperatures. From Fig. 1a, the peaks at  $2\theta = 34.8^\circ$ ,  $33.3^\circ$ ,  $20.7^\circ$ ,  $20.8^\circ$ ,  $32.9^\circ$  are attributed to the  $\beta$ - $\text{AgAl}_{0.4}\text{Ga}_{0.6}\text{O}_2$  (JCPDS 21-1070) and  $2\theta = 36.5^\circ$ ,  $14.5^\circ$ ,  $29.2^\circ$ ,  $38.8^\circ$ ,  $42.3^\circ$  are ascribed to the  $\alpha$ - $\text{AgAl}_{0.4}\text{Ga}_{0.6}\text{O}_2$  (JCPDS 84-2201). The obtained samples present the sharp diffraction peaks, indicating that two samples are pure phase and have high degree of crystallinity, respectively [22]. When the hydrothermal reaction temperature rises to 90 °C, besides the peaks of  $\beta$ - $\text{AgAl}_{0.4}\text{Ga}_{0.6}\text{O}_2$ , some additional diffraction peaks corresponding to  $\alpha$ - $\text{AgAl}_{0.4}\text{Ga}_{0.6}\text{O}_2$  are observed. This suggests that part of the  $\beta$ - $\text{AgAl}_{0.4}\text{Ga}_{0.6}\text{O}_2$  has transformed into the  $\alpha$ - $\text{AgAl}_{0.4}\text{Ga}_{0.6}\text{O}_2$ . The low intensity of the peaks is due to the relatively low weight proportion of  $\alpha$  phase in the heterostructure. With increasing the hydrothermal reaction temperature to 100 °C, the intensity of main peak of the  $\alpha$ - $\text{AgAl}_{0.4}\text{Ga}_{0.6}\text{O}_2$  is close to that of the  $\beta$ - $\text{AgAl}_{0.4}\text{Ga}_{0.6}\text{O}_2$ , showing that more  $\beta$ - $\text{AgAl}_{0.4}\text{Ga}_{0.6}\text{O}_2$  has converted into the  $\alpha$ - $\text{AgAl}_{0.4}\text{Ga}_{0.6}\text{O}_2$ . While the hydrothermal reaction temperature reaches 110 °C, the intensive diffraction peaks of the  $\alpha$ - $\text{AgAl}_{0.4}\text{Ga}_{0.6}\text{O}_2$  can be

Download English Version:

<https://daneshyari.com/en/article/7117494>

Download Persian Version:

<https://daneshyari.com/article/7117494>

[Daneshyari.com](https://daneshyari.com)